15th Triennial World Congress, Barcelona, Spain

OPTIMAL CONTROL THEORY APPLIED TO HYBRID FUEL CELL POWERED VEHICLE

G. Paganelli [1], T.M. Guerra [2], S. Delprat [2]
Y. Guezennec [1], G. Rizzoni [1]

[1] Center for Automotive Research - Ohio State University
930 Kinnear Road ,Columbus, Ohio 43212 - USA
[2] LAMIH UMR CNRS 8530 - Université de Valenciennes et du Hainaut Cambrésis
le Mont Houy 59313 Valenciennes CEDEX 9 - France

Abstract: This paper focuses on the energy management control strategy for a hybrid fuel cell powered vehicle. A method based on optimal control theory is presented. This control strategy has been applied to a representative hybrid PEM (Proton Exchange Membrane) fuel cell mid-size vehicle. Simulation results on *a priori* known driving cycle are presented and compared to a sub-optimal strategy. *Copyright © 2002 IFAC*

Keywords: Hybrid vehicles, Energy management systems, Optimal control, Optimal power flow, Fuel cell.

1. INTRODUCTION

Fuel cell powered vehicles are foreseen as an answer to the rising concerns for the environment. The hybridization of a fuel cell powered vehicle may be required for start-up, cold-start response or fuel cell cost, weight and volume considerations. An other reason for hybridization is the opportunity for energy efficiency improvement. Actually, the additional energy storage device allows kinetic energy recovery and energy management optimization opportunity by offering an extra degree of freedom in the power flow. This creates the need for a higher level of control in the vehicle, typically referred to as the supervisory controller or control strategy. Commonly used hybrid fuel cell control strategy are the SOC-based control, the load following or a combination of both (Boettner, *et al.*, 2001, Ogburn, *et al.*, 2000, Patton, *et al.*, 2001). While generally allowing proper operation, those approaches do not embed any energy minimization consideration and consequently do not reach optimal fuel economy.

Regardless of the topology of an hybrid powertrain, the essence of the control problem is the instantaneous management of the power flows from both power sources to achieve the overall minimum fuel consumption. The global nature of both the objective (hydrogen consumption) and the constraint (accumulator state-of-charge) does not lend itself to traditional global optimization technique, as the future is unknown in actual driving circumstances. A previous work (Paganelli *& al*. 2002) led to a Hybrid Fuel cell control strategy that instantaneously optimizes the power split between the energy converters, while somehow accounting for the global nature of the problem. The proposed power split algorithm, *Equivalent Consumption Minimization Strategy* (ECMS) was based on a heuristic formulation of the power flow within the electrical accumulator. Although suitable for real time application and yielding very good fuel economy, this heuristic approach does not allow to reach the global optimal power flow distribution.

The approach presented in this paper proposes to bridge this gap. The objective of this work is thus to determine the global optimal power flow distribution, in terms of energy management, within an hybrid fuel cell powered vehicle. It is an extension of a previously developed method to apply optimal control theory to a parallel hybrid electric/ICE engine vehicle (Delprat, *et al*., 2001a).

2. FUEL CELL SYSTEMS

Most typically, the architecture of a hybrid fuel cell vehicle includes a DC bus physically represented by the electrical accumulator. It is connected to the fuel cell via a DC/DC converter on one side and to the electric machine with an associated converter on the other side, as shown in Figure 1.

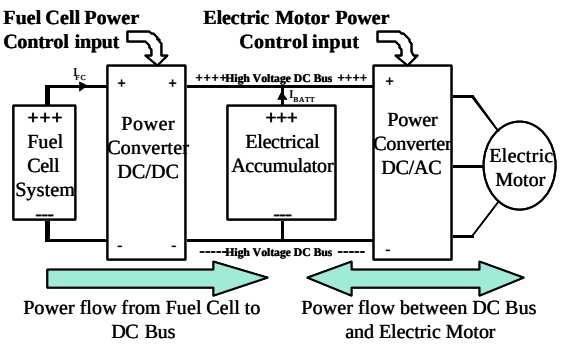

Fig. 1. General Hybrid Fuel Cell System

The approach presented in this paper could easily be applied to any kind of fuel cell hybrid powertrain. As a representative example, a Proton Exchange Membrane Fuel Cell stack is assumed. The design and operating parameters used are representative of those proposed in automotive application for a mid-size SUV-type vehicle, they are shown in Table 1.

Table 1: Fuel Cell Stack operating Parameters

Input Parameter	Value
Active Area [cm^2]	400
Number of cells in series	440
Nominal operating temperature [K]	353
Air and hydrogen inlet temperature [K]	333
Air and hydrogen inlet relative humidity [%]	100
Anode pressure [atm]	2
Fuel utilization	0.8
Ambient temperature [K]	273
Air/Fuel Stoichiometric Ratio [kmol air /kmol h2]	2
System Maximum Net Power at Nominal Operating Temperature [kW]	86.4

This representative fuel cell system has been simulated using a hybrid fuel cell vehicle model developed at the Ohio State University for its VP-SIM vehicle performance simulator (Boettner, *et al.*, 2002). It is based on a semi-empirical pressure and temperature dependant piecewise fuel cell voltage modelling.

It is assumed the auxiliaries consist in a variable speed compressor/expander for the air delivery system, a pump/heat-exchanger/fan for the cooling system, a pump for hydrogen recirculation and water pumps for humidification. All the auxilaries are controlled to ideally track the fuel cell system power demand with constant stoichiometric ratios and are assumed to be powered by the fuel cell itself. The net system power being the remaining power available. The compressor is the greatest auxiliary consumer with a maximum power needed of 23 kW, assuming an isentropic efficiency ranging from 53 to 71%. We consider here the entire system consisting of the fuel cell with its auxiliaries and we are interested in the net power out of this system. As shown in Figure 2, the maximum model based net power available from the fuel cell system is related to the stack temperature, it reaches a maximum of 86.4 kW at nominal operating temperature (80°C or 353k).

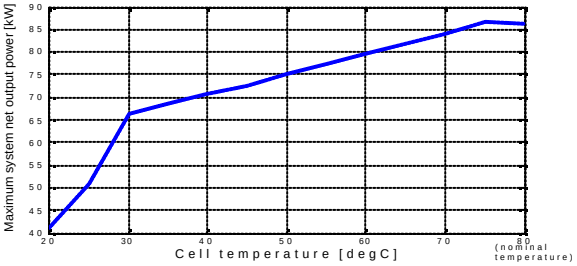

Fig. 2. VP-SIM computed Maximum system output power available function of stack temperature

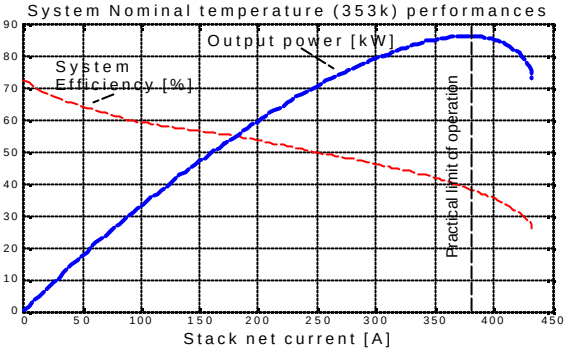

Fig. 3. VP-SIM computed net Fuel cell system output power and efficiency function of net output current at nominal temperature

As depicted in Figure 3 for the particular case of nominal temperature, the system output power increases along with net output current up to a certain limit where the maximum output power operating point is reached. This limit is due to a more significant drop of output voltage and must be the practical limit of operation of the system. Clearly above this point more hydrogen is consumed for less output power inducing a dramatic efficiency drop. The efficiency shown is computed on the basis of the net system output power versus enthalpy input to the system, *i.e.* mass flow of hydrogen consumed times hydrogen LHV (Lower Heating Value). The efficiency remains high on the all range of operation, this can be mainly explained by the presence of an expander and by the compressor being controlled to satisfy a constant air stoichiometric ratio, which is an ideal case but not always practically realisable, especially for low loads.

In a pure fuel cell vehicle, the fuel cell power has to track the driver demand. With a hybrid configuration, the fuel cell remains the only component to provide the net energy, the buffer role of the additional energy storage device allows flexibility in the choice of the fuel cell operating point "trajectory" to provide this needed amount of energy. One can foresee that for a given amount of power produced by the fuel cell system over a driving cycle, different fuel cell operating point "trajectories" might lead to completely different overall fuel consumption. This is due to the large possible excursion of the fuel cell efficiency. An other reason is the operating point "trajectory" impacts also on the stack temperature, which in turn significantly affects the fuel cell performance (efficiency and available power). The purpose of the following approach is to define the optimal operating point trajectory of this highly coupled system to reach the minimum overall fuel consumption.

3. OPTIMAL CONTROL FORMULATION

3.1. Control strategy of a hybrid fuel cell vehicle

The aim of a hybrid control strategy is how to instantaneously distribute the power on both energy sources, electrical accumulator and fuel cell system,

to satisfy the road load power requirement while meeting the instantaneous and global constraints and objectives. In our case the road load power requirement is the power requested by the traction electric motor at time t : $P_{em}(t)$ positive or negative. In a real vehicle it is continuously given by the driver through the gas pedal, and prorated in function of the maximum power available at the current vehicle speed. Both the battery and the fuel cell system contribute to provide this power:

$$P_{em}(t) = P_{batt}(t) + P_{fc}(t) \quad (1)$$

Where $P_{fc}(t)$ is the net power produced by the fuel cell and $P_{batt}(t)$ is the power to/from the electrical accumulator[1].

Practically, the power distribution is adjusted by controlling the power produced by the fuel cell $P_{fc}(t)$ through the associated power converter shown on figure 1. The power produced (or captured) by the electrical accumulator $P_{batt}(t)$ being the remaining power needed to satisfy the total power requirement: $P_{batt}(t) = P_{em}(t) - P_{fc}(t)$

The chosen control variable to adjust the fuel cell power is the net current produced by the Fuel Cell system $I_{net}(t)$. This is the available current output of the system, *i.e.*, the current produced by the fuel cell less the current drawn by its auxiliaries.

The considered dynamic variables of the system are the battery state of charge (SOC) and the fuel cell stack temperature. They are described by the following system of equations:

$$\begin{cases} SOC(t+1) = SOC(t) + \left(P_{fc}(t) - P_{em}(t)\right) \cdot Eff_{batt} \cdot Te \\ T_{fc}(t+1) = a \cdot T_{fc}(t) + Q(I_{net}(t),\ T_{fc}(t)) \cdot Te \end{cases} \quad (2)$$

Where :

- $SOC(t)$ is the State of Charge at time t;
- $P_{fc}(t)$ is the net power produced by the fuel cell system at time t;
- Eff_{batt} is the battery efficiency dependant of power flow direction ;
- $T_{fc}(t)$ is the fuel cell stack internal temperature at time t;
- Te is the sampling time;
- a represents the natural heat exchange coefficient, it depends of the ambient temperature;
- $Q(I_{fc\_net}(t), T_{fc}(t))$ is the heat produced by the stack function of net current $I_{fc\_net}(t)$ and stack temperature $T_{fc}(t)$.

[1] Various efficiencies have been neglected in this paper for clarity, but are included in the formulation of the control strategy actually implemented.

As can be seen in the above set of equation 2, the electrical accumulator state of charge $SOC(t)$ is a pure integration process. The temperature $T_{fc}(t)$ is modelled as a simplified first order response type system.

The chosen relevant criterion is the fuel (hydrogen) consumption on a temporal window of N samples. The criterion can be written as :

$$J = \sum_{t=0}^{N-1} \dot{m}_f\left(I_{net}(t),\ T_{fc}(t)\right) \cdot Te \quad (3)$$

$\dot{m}_f(I_{net}(t),\ T_{fc}(t))$ represents the hydrogen consumption (in gr/s) required to produce the current $I_{net}(t)$ at the temperature $T_{fc}(t)$.

In the following sub-sections, an approach based on optimization control tools (Borne, *et al.*, 1990) is proposed.

3.2. Formulation of the optimization problem

The power produced by the fuel cell system is derived from the product of current and voltage available on the system output:

$$P_{fc}(t) = I_{net}(t) \cdot V_{fc}\left(I_{net}(t), T_{fc}(t)\right) \quad (4)$$

To simplify notation, let us define $F\left(I_{net}(t), T_{fc}(t)\right)$ representing the voltage on the fuel cell system output with a $(Eff_{batt} \cdot Te)$ multiplicative factor:

$$F\left(I_{net}(t), T_{fc}(t)\right) \triangleq V\left(I_{net}(t), T_{fc}(t)\right) \cdot Eff_{batt} \cdot Te \quad (5)$$

It comes:

$$P_{fc}(t) \cdot Eff_{batt} \cdot Te \triangleq I_{net}(t) \cdot F\left(I_{net}(t), T_{fc}(t)\right) \quad (6)$$

The following definition is also used :

$$f\left(x(t), I_{net}(t)\right) \triangleq \begin{bmatrix} SOC(t) - P_{em}(t) \cdot Eff_{batt} \cdot Te \\ \quad + I_{net}(t) \cdot F\left(I_{net}(t), T_{fc}(t)\right) \\ a \cdot T_{fc}(t) + Q\left(I_{net}(t), T_{fc}(t)\right) \cdot Te \end{bmatrix} \quad (7)$$

with the state vector :

$$x(t) = \begin{bmatrix} SOC(t) & T_{fc}(t) \end{bmatrix}^T \quad (8)$$

The power distribution on both energy sources can be written as an optimization under constraints problem:

System $$x(t+1) = f\left(x(t), I_{net}(t)\right) \quad (9)$$

Criterion $$J = \sum_{t=0}^{N-1} \dot{m}_f\left(I_{net}(t),\ T_{fc}(t)\right) \cdot Te \quad (10)$$

Constraint $$SOC(N) = SOC(0) \quad (11)$$

Introducing the lagrangian parameters vector $l(t) = \begin{bmatrix} l_1(t) & l_2(t) \end{bmatrix}^T$ leads to the minimization of :

$$J = \sum_{t=0}^{N-1} \{\dot{m}_f\left(I_{net}(t), T_{fc}(t)\right) \cdot Te + l(t) \cdot \left(x(t+1) - f\left(x(t), I_{net}(t)\right)\right)\} \quad (12)$$

First order conditions:

$$\frac{\partial J'}{\partial SOC} = \left[l_1(t-1) - l_1(t) \right] = 0$$

$$\frac{\partial J'}{\partial T_{fc}} = \left[l_2(t-1) - l_2(t) \cdot \left(a + \frac{\partial Q\left(I_{net}(t), T_{fc}(t)\right)}{\partial T_{fc}(t)} \right) - l_1(t) \cdot I_{net}(t) \cdot \frac{\partial F\left(I_{net}(t), T_{fc}(t)\right)}{\partial T_{fc}(t)} \right] = 0 \quad (13)$$

Then : $\forall t,\ l_1(t) = l_1(0)$ and :

$$l_2(t)\left(a + \frac{\partial Q\left(I_{net}(t), T_{fc}(t)\right)}{\partial T_{fc}(t)} \right) = l_2(t-1) - l_1(0) \cdot I_{net}(t) \cdot \frac{\partial F\left(I_{net}(t), T_{fc}(t)\right)}{\partial T_{fc}(t)} \quad (14)$$

$$\frac{\partial J'}{\partial I_{net}(t)} = \frac{\partial \dot{m}_f\left(I_{net}(t)\right)}{\partial I_{net}(t)} - l_1(0) \cdot I_{net}(t) \cdot \frac{\partial F\left(I_{net}(t), T_{fc}(t)\right)}{\partial I_{net}(t)} - l_1(0) \cdot F\left(I_{net}(t), T_{fc}(t)\right) - l_2(t) \cdot \frac{\partial Q\left(I_{net}(t), T_{fc}(t)\right)}{\partial T_{fc}(t)} \quad (15)$$

Computation of solution with respects to (14) and (15) requires analytical expression of the hydrogen consumption, the heat produce by the stack and output voltage. The VP-SIM fuel cell model allows computing of the needed variables with a very good accuracy. Nevertheless, due to the complexity and the non-linearity of the equations involved in this model some approximations have been performed.

3.3. Approximation of characteristics

Computed output voltage curves are shown on figure 4, they are highly related to the current with a steeper decreasing rate at low temperature.

As defined in equation (5), $F\left(I_{net}(t), T_{fc}(t)\right)$ is linearly related to the fuel cell system output voltage characteristics $V\left(I_{net}(t), T_{fc}(t)\right)$.

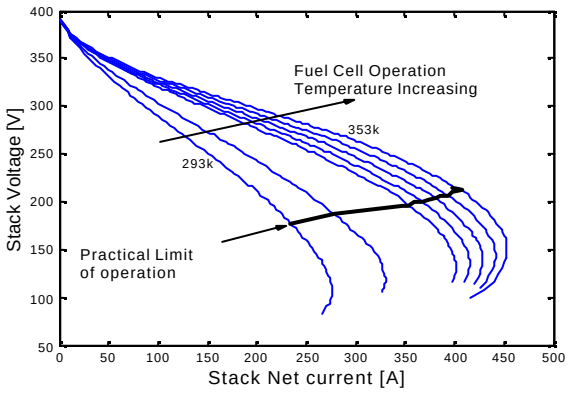

Fig. 4. VP-SIM computed fuel cell system output voltage

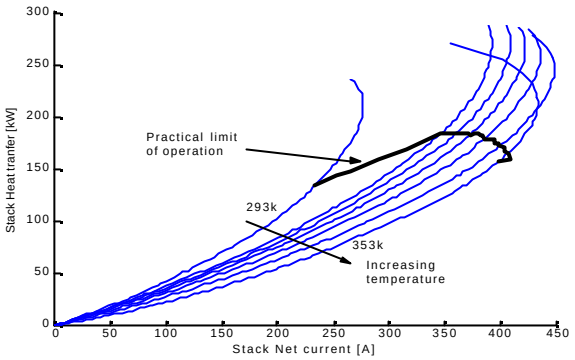

Fig. 5. VP-SIM computed heat transfer curves

The VP-SIM model uses conservation of energy analysis to compute the heat transfer associated with the fuel cell, $Q\left(I_{net}(t), T_{fc}(t)\right)$.

As shown by the curves on figure 5, the operation of a fuel cell is essentially exothermic [2].

Linear piecewise approximation of the characteristics Q and V provides the required analytical expression of $F\left(I_{net}(t), T_{fc}(t)\right)$ and $Q\left(I_{net}(t), T_{fc}(t)\right)$ to solve (14) and (15). Let n be the number of models obtained, each of them being defined on a segment $\left[\mathrm{I}^i_{\min}, \mathrm{I}^i_{\max}\right]$, $i \in \{0,\ldots,n-1\}$, with of course $\mathrm{I}^0_{\min} = 0, \mathrm{I}^{n-1}_{\max} = \mathrm{I}_{\max}\left(T_{fc}(t)\right)$:

$$F^i\left(I_{net}, T_{fc}\right) = a^i\left(T_{fc}\right) \cdot I_{net} + b^i\left(T_{fc}\right) \quad (16)$$

$$Q^i\left(I_{net}, T_{fc}\right) = c^i\left(T_{fc}\right) \cdot I_{net} + d^i\left(T_{fc}\right) \quad (17)$$

According to the electrochemical inner reaction of a fuel cell, the mass flow of hydrogen consumed is linearly related to the current drawn at the stack level I_{fc}:

$$\dot{m}_f(t) = K \cdot I_{fc}(t) \quad (18)$$

where K is a constant function of the fuel cell active area, the Faraday's constant and the molecular weight of hydrogen.

When expressing the mass flow function of the net fuel cell current I_{net} as opposed to stack current, a slight non-linearity appears due to the non-linear nature of the current drawn by the auxiliaries. Nevertheless, as shown on figure 6, this non-linearity is only relevant at high current and especially above the practical limit of operation.

Since the operating point of the system must never exceed the practical limit of operation, for the purpose of this study the hydrogen mass flow is defined as a linear function of the stack net output current:

$$\dot{m}_f(t) \triangleq K' \cdot I_{net}(t) \quad (19)$$

[2] The heat transfer is defined positive when it flows from the system to the environment.

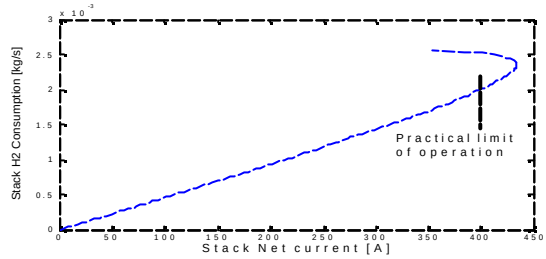

Fig. 6. VP-SIM computed stack hydrogen consumption versus stack net current at nominal temperature

The next sub-section proposes a solution to the optimization problem using those approximations.

3.4. Towards an optimal solution

Using (14) and (15) with (16) and (17), and after some easy calculus we found the following second order equation to be solved at each sampling time :

$$I_{net}^2(t)\cdot l_1(0)\cdot\left(c^i\left(T_{fc}(t)\right)\frac{\partial a^i\left(T_{fc}(t)\right)}{\partial T_{fc}(t)}-2a^i\left(T_{fc}(t)\right)\frac{\partial c^i\left(T_{fc}(t)\right)}{\partial T_{fc}(t)}\right)$$
$$+I_{net}(t)\cdot\left(l_1(0)\left\{c^i\left(T_{fc}(t)\right)\frac{\partial b^i\left(T_{fc}(t)\right)}{\partial T_{fc}(t)}-b^i\left(T_{fc}(t)\right)\frac{\partial c^i\left(T_{fc}(t)\right)}{\partial T_{fc}(t)}\right.\right.$$
$$\left.-2a^i\left(T_{fc}(t)\right)\left(a+\frac{\partial d^i\left(T_{fc}(t)\right)}{\partial T_{fc}(t)}\right)\right\}+\frac{\partial \dot m_f\left(I_{net}(t)\right)}{\partial I_{net}(t)}\frac{\partial c^i\left(T_{fc}(t)\right)}{\partial T_{fc}(t)}\Bigg)$$
$$+\left(a+\frac{\partial d^i\left(T_{fc}(t)\right)}{\partial T_{fc}(t)}\right)\cdot\left(\frac{\partial \dot m_f\left(I_{net}(t)\right)}{\partial I_{net}(t)}-l_1(0)b^i\left(T_{fc}(t)\right)\right)$$
$$-l_2(t-1)\cdot c^i\left(T_{fc}(t)\right)=0 \qquad (20)$$

At last, one can see that the initial values of the lagrangian parameters, i.e. $l(0)=\left[\,l_1(0)\quad l_2(0)\,\right]^T$ are enough to compute an optimal solution with respect to (9)~(11) (Borne, *et al.*, 1990). Clearly, the final state of charge depends only on the initial values of the lagrangian parameters. A simple gradient descent is used to obtain $l_1(0)$ and $l_2(0)$ which enforce $x(N)=x(0)$.

4. SIMULATION RESULTS

In the following application, the fuel cell system considered above is associated to a 42 kW maximum power nickel metal hydride battery with typical specific power of 500 W/kg and specific energy of 50 Wh/kg. This configuration is the result of a sensitivity analysis presented in (Boettner, *et al.*, 2001) and is suitable for the SUV-type vehicle specifications presented in table 2. It is powered by an AC induction electric motor, requiring up to 126 kW.

Table 2: Simulated Vehicle Specifications

Mass [kg]	2360
Frontal area [m^2]	4
Coefficient of drag	0.75
Coefficient of rolling resistance	0.015

The 1380 seconds long Federal Urban Driving Schedule (FUDS) was used for the simulations conducted with the VP-SIM simulator. The fuel cell starts at ambient temperature to represent a cold start. The initial battery state-of-charge is 0.7.
The process leading to optimal results is thus:

1. Using the VP-SIM simulator, compute the power required by the electric motor to meet the driving schedule $P_{em}(t), t\in[0...1380]$;
2. Input the obtained power needed vector into the optimal control algorithm described above to get an optimal fuel cell net current distribution $I_{net}(t), t\in[0...1380]$;
3. Implement this fuel cell net current distribution into the VP-SIM simulator.

Let's emphasize that, at step 2, the optimal current control law $I_{net}(t)$ is computed using an approximated model according to equations 16 to 19. At step 3, this control law is then implemented into a more complex and accurate model, which gives a slightly different result from the one computed with the optimal control algorithm. Nevertheless, experiences have shown that improvement of the accuracy of the simplified model leads to a significant increase of the algorithm complexity for very little improvement.

The solid lines on figure 7 show the simulated system behaviour under the optimal current law for the FUDS driving cycle.

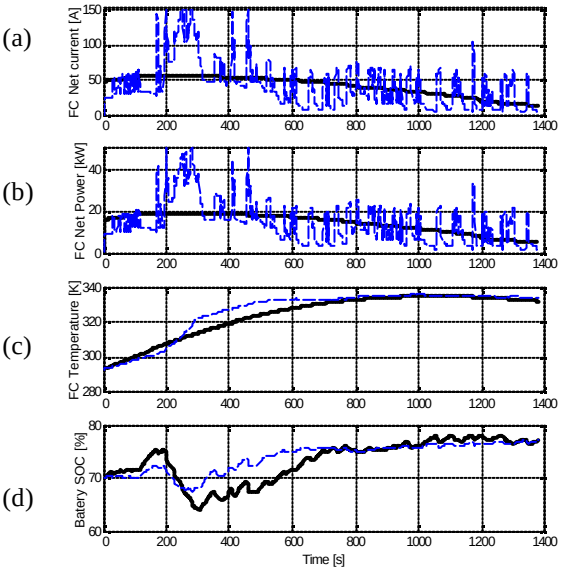

Fig. 7. Simulated results with optimal control on FUDS cycle

In order to evaluate and contrast the results of the optimal control theory approach, the well-proofed ECMS local optimization strategy (Paganelli, et al., 2002) is used as a basis of comparison. The dashed lines show the corresponding ECMS results. As can be seen, the current law provided by the optimal control, plot (a), is significantly smoother. Consequently, the fuel cell power and temperature, plot (b) and (c), exhibit much less excursion. Nevertheless, the plot (d), shows that the battery state of charge ends at the same level in both cases.

Table 3 below gives the compared fuel economy results. The fuel usage is corrected for (minor) differences in initial and final battery state-of-charge. The correction is based on the net electricity used (reflected by the difference between battery final state of charge and initial state of charge), using the corresponding average fuel cell system efficiency from that simulation to convert net electricity usage to equivalent fuel consumption. Furthermore, the hydrogen usage is converted to equivalent gasoline usage based on the relative lower heating value of hydrogen and gasoline. This allows to report the results in a more "intuitive" form. An improvement of more than 3% is achieved with the optimal control approach.

Table 3 FUDS simulated fuel economy

	Hydrogen used	Gasoline equivalent fuel consumption
ECMS	267.1 g	8.14 l/100km (28.86 mpg)
Optimal Control	257.7 g	7.85 l/100km (29.92 mpg)

5. CONCLUSION

This paper describes a formulation based on the optimal control theory for the supervisory control in charge-sustaining hybrid fuel cell vehicles on *a priori* known driving cycle. This method allows to define the optimal power split between the fuel cell and the electrical accumulator to globally minimize the overall hydrogen consumption. The use of optimal control theory reduces the computation cost in comparison with other optimization methods. For one specific representative simulated hybrid fuel cell vehicle configuration, the proposed control strategy outperforms the fuel economy results obtained with other control strategies while enforcing a charge-sustaining operation. Nevertheless, this approach is not limited to the battery/fuel cell configuration presented in this paper, it can easily be applied to other configurations such as ultracapacitor/fuel cell.

Although not dramatic improvement in fuel efficiency is achieved in comparison with the ECMS control strategy for the presented simulated driving cycle, this approach provides an optimal reference result for off-line assessment of other strategies. Implementing the result of the proposed approach for real time control would require the forecast of a correct value of the lagrangian parameters, i.e. $l(0)$, which will provide an acceptable state of charge at the end of the mission. Clearly if the trip is not *a priori* known, it is impossible to forecast this value and to directly use the proposed approach for real time control. Nevertheless, as shown in (Delprat, *et al*., 2001b), $l(0)$ has a monotonic effect on state of charge variation. Therefore adjusting the value of $l(0)$ during real time operation, using a simple PI controller for example, allows to sustain the state of charge close to a target value. Future work will be devoted to this real time adaptation of the proposed method.

REFERENCES

Boettner D., G. Paganelli, Y. Guezennec, G. Rizzoni, M. J. Moran (2002). Proton Exchange Membrane (PEM) fuel cell system model for automotive vehicle simulation and control. ASME *Journal of Energy Resources Technology*, Volume 124, pp.1-8, March 2002.

Boettner D., G. Paganelli, Y. Guezennec. M. J. Moran, G. Rizzoni (2001). Component Power Sizing and Limits of Operation for Proton Exchange Membrane (PEM) Fuel Cell/Battery Hybrid Automotive Applications. *ASME - International Mechanical Engineering Congress and Exposition* – IMECE2001/DSC-24524 - New York, November 2001.

Borne P., G. Dauphin-tanguy, J.P. Richard, F. Rotella, I. Zambettakis (1990). *Systems control and optimization*. Méthodes et Techniques de l'ingénieur, Éditions Technip (in french).

Delprat S., T.M. Guerra, G. Paganelli, J. Lauber, M. Delhom (2001a). Control strategy optimization for an hybrid parallel powertrain - Presented to the *ACC'2001, American Control Conference* Crystal Gateway Marriott, Arlington, VA, USA - June 2001, pp. 1315-1320.

Delprat S., T.M. Guerra, J. Rimaux (2001b). Optimal control of a parallel powertrain : From global optimization to real time control strategy, *Electric Vehicle Symposium, EVS18*, Berlin, October 2001.

Ogburn M., D.J. Nelson, W. Luttrell, B. King, S. Postle, R. Fahrenkrog (2000). Systems Integration and Performance Issues in a Fuel Cell Hybrid Electric Vehicle. *SAE*, Paper #2000-01-0376.

Paganelli G., Y. G. Guezennec, G. Rizzoni (2002). Optimizing System Control Strategy for Hybrid Fuel Cell Vehicle. Paper 2002-01-0102 – SP1691 - *SAE 2002 World Congress*, Detroit, Michigan, USA - March 4-7, 2002.

Patton D., J. Latore, M. Ogburn, S. Gurski, P. Bryan, D. J. Nelson (2001). Design and Development of the 2000 Virginia Tech Fuel Cell Hybrid Electric FutureTruck. *Society of Automotive Engineers SAE* SP-1617, pp.185-202.